JCTC Journal of Chemical Theory and Computation

Article

pubs.acs.org/JCTC

Benchmark Study of Density Cumulant Functional Theory: Thermochemistry and Kinetics

Andreas V. Copan,* Alexander Yu. Sokolov, and Henry F. Schaefer III

Center for ComputationalQuantum Chemistry, The University of Georgia, Athens, Georgia 30602, United States

Supporting Information

ABSTRACT: We present an extensive benchmark study of density cumulant functional theory (DCFT) for thermochemistry and kinetics of closed- and open-shell molecules. The performance of DCFT methods (DC-06, DC-12, ODC-06, and ODC-12) is compared to that of coupled-electron pair methods ($CEPA_0$ and $OCEPA_0$) and coupled-cluster theory (CCSD and CCSD(T)) for the description of noncovalent interactions (A24 database), barrier heights of hydrogen-transfer reactions (HTBH38), radical stabilization energies (RSE30), adiabatic ionization energies (AIE), and covalent bond stretching in diatomic molecules. Our results indicate that out of four DCFT methods the ODC-12 method is the most reliable and accurate DCFT formulation to date. Compared to CCSD, ODC-12 shows superior results for all benchmark tests employed in our study. With respect to coupled-pair theories, ODC-12 outperforms $CEPA_0$ and shows similar accuracy to the orbital-optimized $CEPA_0$ variant ($OCEPA_0$) for systems at equilibrium geometries. For covalent bond stretching, ODC-12 is found to be more reliable than $OCEPA_0$. For the RSE30 and AIE data sets, ODC-12 shows competitive performance with CCSD(T). In addition to benchmark results, we report new reference values for the RSE30 data set computed using coupled cluster theory with up to perturbative quadruple excitations.

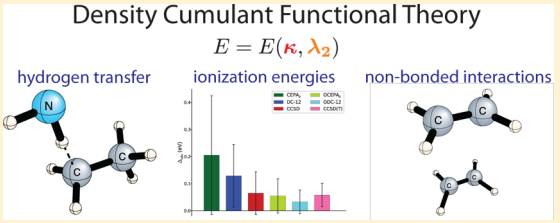

INTRODUCTION

Recent developments in ab initio quantum chemistry have resulted in a variety of computational models for studying molecules. Apart from concerns about efficiency and accuracy, several concepts have evolved as criteria for judging the merits of a particular method. Energy-based criteria typically define an "ideal" approximation as one yielding correlation energies that are size-consistent, extensive,[1] well-defined (giving continuous, unique potential surfaces), and variational.[2] While it has been argued that the practical benefits of variationality are rather limited,[3] the efficiency of gradient computations, at least, is improved by formulating a theory in terms of a Hermitian and stationary energy functional.[4] With respect to scope and stability, methods that show consistent performance for open-shell systems, strongly correlated states, and nonequilibrium geometries are particularly valuable.[3]

The incorrect scaling of truncated configuration interaction (CI) energies with system size has inspired the development of size-extensive alternatives. Among the earliest formulations, the coupled electron pair approximations (CEPAs)[5−9] attracted much attention in the 1970s,[10−14] offering rigorous extensivity and size-consistency while retaining much of the linearity[15] of CI in their equations. CEPA methods, however, have been shown to rapidly deteriorate as the molecular geometry deviates from equilibrium[15] and yield energies that vary under the rotation of the occupied orbitals.[8] Partly in light of such defects, CEPA has been largely displaced by coupled-cluster (CC) theory.[3,16−22] In addition to size-extensivity, CC offers orbital invariance and improved stability for nonequilibrium structures[15] but has a non-Hermitian energy functional and nonlinear equations which are not readily amenable to parallel implementation. Although neither class of methods is strictly variational, VCEPA (variational CEPA) has been shown to be effectively equivalent to its nonvariational counterpart.[23] Various other modifications to resolve the deficiencies of traditional CEPA have been explored, including self-consistent size-consistent CI,[24,25] orbital-invariant CEPA,[26,27] and orbital-optimized CEPA formulations.[28−31] Recently, the CEPA methods have been revived by Neese and co-workers[23,32,33] who developed the local pair-natural-orbital CEPA (LPNO-CEPA) methods and have implemented them for massively parallel computer architectures.

It has recently been demonstrated[34−37] that CEPA methods naturally arise in the context of theories that obtain the molecular energies from density cumulants, the connected and extensive components of the reduced density matrices (RDMs).[38−43] The advantage of cumulant-based theories is that, unlike their RDM-based counterparts,[44−46] they are naturally size-extensive and size-consistent.[41,47] We have recently achieved the first implementation[48,49] of density cumulant functional theory (DCFT), proposed by Kutzelnigg in 2006.[34] In DCFT, the molecular energy is obtained in terms of a mean-field one-particle RDM and the two-particle density cumulant, constrained to be at least approximately N-representable (i.e., to correspond to a physical N-electron

Received: April 3, 2014

   dx.doi.org/10.1021/ct5002895 | J. Chem. Theory Comput. XXXX, XXX, XXX−XXX

Table 1. Errors in Interaction Energies (kcal mol^{-1}) for 24 Noncovalently Bound Molecular Dimers Comprising the A24 Database[60] Computed Using Seven Methods with the aug-cc-pVTZ Basis Set[a]

	complex	sym	ΔCEPA$_0$	ΔDC-06	ΔDC-12	ΔCCSD	ΔOCEPA$_0$	ΔODC-06	ΔODC-12	E_{ref} [CCSD(T)]
1	$H_2O\cdots NH_3$	C_S	0.26	0.24	0.22	0.36	0.19	0.20	0.18	−7.18
2	$H_2O\cdots H_2O$	C_S	0.19	0.18	0.16	0.25	0.13	0.14	0.12	−5.71
3	HCN···HCN	C_S	0.21	0.27	0.16	0.15	0.18	0.26	0.14	−7.12
4	HF···HF	C_S	0.14	0.13	0.11	0.16	0.08	0.09	0.07	−5.20
5	$NH_3\cdots NH_3$	C_{2h}	0.15	0.13	0.14	0.26	0.12	0.12	0.12	−3.43
6	$HF\cdots CH_4$	C_{3v}	0.17	0.16	0.20	0.23	0.12	0.12	0.16	−2.30
7	$NH_3\cdots CH_4$	C_{3v}	0.07	0.05	0.05	0.13	0.05	0.05	0.04	−1.08
8	$H_2O\cdots CH_4$	C_S	0.06	0.05	0.04	0.11	0.05	0.05	0.04	−1.03
9	$CH_2O\cdots CH_2O$	C_S	0.89	0.99	0.65	0.46	0.62	0.87	0.46	−5.23
10	$H_2O\cdots C_2H_4$	C_S	0.15	0.16	0.15	0.31	0.20	0.26	0.21	−3.33
11	$CH_2O\cdots C_2H_4$	C_S	0.21	0.18	0.14	0.27	0.19	0.24	0.16	−2.24
12	HCCH···HCCH	C_{2v}	0.07	0.05	0.05	0.20	0.10	0.12	0.10	−2.57
13	$NH_3\cdots C_2H_4$	C_S	0.09	0.06	0.08	0.24	0.12	0.15	0.13	−2.07
14	$C_2H_4\cdots C_2H_4$	C_{2v}	0.10	0.02	0.07	0.33	0.14	0.13	0.15	−1.81
15	$CH_4\cdots C_2H_4$	C_S	0.02	−0.02	0.01	0.14	0.05	0.04	0.06	−0.92
16	$BH_3\cdots CH_4$	C_S	0.23	0.18	0.24	0.37	0.18	0.16	0.22	−2.52
17	$CH_4\cdots C_2H_4$	C_S	0.13	0.09	0.13	0.23	0.10	0.09	0.09	−1.37
18	$CH_4\cdots C_2H_6$	C_S	0.09	0.06	0.09	0.17	0.07	0.06	0.09	−1.14
19	$CH_4\cdots CH_4$	D_{3d}	0.08	0.06	0.08	0.14	0.06	0.05	0.08	−0.93
20	$Ar\cdots CH_4$	C_{3v}	0.07	0.05	0.07	0.10	0.05	0.05	0.06	−0.78
21	$Ar\cdots C_2H_4$	C_{2v}	0.03	−0.01	0.02	0.11	0.05	0.03	0.05	−0.63
22	$C_2H_4\cdots HCCH$	C_{2v}	−0.02	−0.19	−0.01	0.38	0.07	−0.06	0.11	0.43
23	$C_2H_4\cdots C_2H_4$	D_{2h}	−0.05	−0.30	−0.03	0.43	0.04	−0.16	0.11	0.41
24	HCCH···HCCH	D_{2h}	0.01	−0.09	0.02	0.34	0.10	0.02	0.12	0.91
		Δ_{abs}	0.14	0.16	0.12	0.25	0.13	0.15	0.13	
		Δ_{std}	0.18	0.23	0.13	0.11	0.12	0.18	0.09	

[a]The errors are relative to CCSD(T) reference values (E_{ref}, kcal mol^{-1}) shown in the rightmost column. For each method the mean absolute deviations from CCSD(T) (Δ_{abs}, kcal mol^{-1}) and the standard deviations from the mean signed error (Δ_{std}, kcal mol^{-1}) are also shown.

wave function). Like traditional CC theory, DCFT is size-extensive and orbital-invariant, but it has the additional advantage of a stationary and Hermitian energy functional, which simplifies the computation of molecular properties. In the original DCFT formulation (DC-06)[34,48,49] N-representability conditions derived from second-order Møller-Plesset perturbation theory (MPPT) were used,[50] yielding equations similar to those of the simplest CEPA model (CEPA$_0$),[7,9] but including higher-order terms in the description of one-particle correlation effects. Using the same set of conditions, we have developed new formulations of DCFT that take advantage of an improved description of the one-particle density matrix (DC-12)[51] and full orbital optimization (ODC-06 and ODC-12 methods).[52]

Our previous studies[48,49,51,52] demonstrated for a limited set of systems that the DC-06, DC-12, ODC-06, and ODC-12 methods generally yield molecular energies and properties competitive with those obtained by CCSD and CCSD(T) but may exhibit unstable performance due to imbalances in the description of electron correlation. Herein, we present an extensive benchmark of the DCFT methods with respect to thermochemical and kinetic molecular properties, including noncovalent interactions, barrier heights in hydrogen-transfer reactions, radical stabilization energies, and adiabatic ionization energies for challenging electron-dense systems. We conclude our benchmark study by testing the performance of DCFT for covalent bond stretching in diatomic molecules.

OVERVIEW OF DCFT

In this section a short overview of DCFT is presented. For details on the theory the reader is referred to our earlier publications.[48,51,52] In the RDM methods[53] the exact molecular energy is expressed as a functional of the one- and two-particle reduced density matrices, $\boldsymbol{\gamma}_1$ and $\boldsymbol{\gamma}_2$ (1-RDM and 2-RDM):

$$E = h_p^q \gamma_q^p + \frac{1}{2} g_{pq}^{rs} \gamma_{rs}^{pq}, \; [\boldsymbol{\gamma}_1]_q^p \equiv \gamma_q^p, \; [\boldsymbol{\gamma}_2]_{rs}^{pq} \equiv \gamma_{rs}^{pq} \tag{1}$$

In eq 1, h_p^q and g_{pq}^{rs} are the usual one- and two-electron integrals in the orthonormal spin−orbital basis $\{\psi_p\}$ and summation over the repeated indices is implied. Expressing $\boldsymbol{\gamma}_1$ through $\boldsymbol{\gamma}_2$ via the partial trace relation $\sum_r \gamma_{qr}^{pr} = (N-1)\gamma_q^p$, the energy functional (eq 1) can be minimized by varying $\boldsymbol{\gamma}_2$ subject to N-representability constraints. This is the essence of the variational 2-RDM approach.[53]

In DCFT, some of the challenges of the 2-RDM approach are circumvented by expanding $\boldsymbol{\gamma}_2$ in terms of its irreducible components—the 1-RDM and the two-particle cumulant (denoted by $\boldsymbol{\lambda}_2$):

$$\gamma_{rs}^{pq} = \gamma_r^p \gamma_s^q - \gamma_r^q \gamma_s^p + \lambda_{rs}^{pq} \tag{2}$$

In eq 2, $\boldsymbol{\lambda}_2$ describes the correlated part of $\boldsymbol{\gamma}_2$ that cannot be expressed via $\boldsymbol{\gamma}_1$. The cumulant also determines the correlation contribution to $\boldsymbol{\gamma}_1$, allowing the 1-RDM to be decomposed as the sum of an idempotent 1-RDM ($\boldsymbol{\kappa}$) and a correlation correction ($\boldsymbol{\tau}$):

$$\boldsymbol{\gamma}_1 = \boldsymbol{\kappa} + \boldsymbol{\tau} \tag{3}$$

dx.doi.org/10.1021/ct5002895 | J. Chem. Theory Comput. XXXX, XXX, XXX−XXX

The correlation component $\boldsymbol{\tau}$ is fully specified by $\boldsymbol{\lambda}_2$, whereas $\boldsymbol{\kappa}$ is independent of $\boldsymbol{\lambda}_2$. Equations 2 and 3 allow us to write an equivalent energy expression with $\boldsymbol{\kappa}$ and $\boldsymbol{\lambda}_2$ as independent functional parameters:

$$E[\boldsymbol{\kappa}, \boldsymbol{\lambda}_2] = \frac{1}{2}(h_p^q + f_p^q)(\kappa_q^p + \tau_q^p) + \frac{1}{4}\overline{g}_{pq}^{rs}\lambda_{rs}^{pq},$$
$$f_p^q = h_p^q + \overline{g}_{pr}^{qs}(\kappa_s^r + \tau_s^r), \overline{g}_{rs}^{pq} = g_{rs}^{pq} - g_{rs}^{qp} \quad (4)$$

Here, the generalized Fock operator $\boldsymbol{f}$ differs from that of Hartree−Fock theory by the presence of an external potential $\overline{g}_{pr}^{qs}\tau_s^r$ due to electron correlation.[34]

To date, all DCFT formulations make the energy (eq 4) stationary with respect to variations of $\boldsymbol{\lambda}_2$, subject to cumulant N-representability constraints derived from second-order Møller-Plesset perturbation theory (MPPT).[50] To account for orbital relaxation effects, the two earliest DCFT methods, DC-06[34,48,49] and DC-12,[51] determined the orbitals by diagonalizing the generalized Fock operator $\boldsymbol{f}$ defined in eq 4. These two methods differ in their description of 1-RDM N-representability. Whereas DC-06 employs an approximate expression for $\boldsymbol{\tau}$ in terms of $\boldsymbol{\lambda}_2$, DC-12 uses the exact relationship. Recently, we proposed orbital-optimized variants of DC-06 and DC-12 (ODC-06 and ODC-12),[52] which fully account for orbital relaxation effects.

COMPUTATIONAL DETAILS

All computations were performed using the PSI4 package.[54] The results were benchmarked against coupled cluster theory with single and double excitations (CCSD),[20−22] CCSD with perturbative triple excitations [CCSD(T)],[55,56] coupled electron pair approximation zero ($CEPA_0$),[7,9] and the orbital-optimized variant of $CEPA_0$ ($OCEPA_0$).[29] All electrons were correlated in all computations. The cc-pCVXZ[57,58] and aug-cc-pVXZ[59] basis sets (X = T, Q) were used (see text for details). Noncovalent interaction energies, hydrogen-transfer barrier heights, and radical stabilization energies were computed using geometries from the A24,[60] HTBH38,[61] and RSE30[62] benchmark databases, respectively, available in PSI4. Adiabatic ionization energies were computed from neutral and cation geometries optimized at each level of theory, with added harmonic zero-point vibrational energy corrections. Harmonic frequencies were computed by numerical differentiation of analytic energy gradients. Single-point energies were converged to 10^{-8} E_h, while the root-mean-square of the energy gradient was converged to 10^{-6} E_h/a_0 for geometry optimizations.

RESULTS AND DISCUSSION

Noncovalent Interactions. We begin by testing the accuracy of DCFT methods for the description of noncovalent interactions in 24 closed-shell molecular dimers, which are listed in Table 1. These molecular complexes comprise the A24 data set[60] developed by Řezáč and Hobza to include a variety of noncovalent interactions, including hydrogen bonding and $\pi-\pi$ stacking. Although Řezáč and Hobza reported the interaction energies at the CCSD(T) complete basis set (CBS) limit, we use CCSD(T)/aug-cc-pVTZ energies as reference values in order to effectively exclude basis-set incompleteness error from the comparison.

Figure 1 depicts mean absolute deviations (Δ_{abs}) relative to CCSD(T) in the binding energies of $CEPA_0$, $OCEPA_0$, CCSD, and the four DCFT methods (DC-06, DC-12, ODC-06, and ODC-12), as well as the root-mean-square deviation from the average signed error (Δ_{std}). All methods but CCSD give similar Δ_{abs} values (0.14 ± 0.02), and a comparison between $CEPA_0$, DC-06, and DC-12 and their orbital-optimized variants ($OCEPA_0$, ODC-06, and ODC-12) shows negligible 0.01 kcal mol^{-1} differences in each case. CCSD gives a significantly larger Δ_{abs} (0.25 kcal mol^{-1}) than the other methods, exceeding the DC-12 Δ_{abs} by a factor of 2 (0.12 kcal mol^{-1}). The Δ_{std} values are much more sensitive to the choice of method than the Δ_{abs} values and are noticeably affected by orbital optimization. ODC-12 gives the smallest standard deviation (Δ_{std} = 0.09), while the largest value was found for DC-06 (0.23 kcal mol^{-1}). The $OCEPA_0$, ODC-06, and ODC-12 methods (Δ_{std} = 0.12, 0.18, and 0.09 kcal mol^{-1}, respectively) exhibit much more consistent performance than their non-orbital-optimized analogues, with Δ_{std} smaller by 0.05 ± 0.01 in each case. CCSD also exhibits a relatively small Δ_{std} value (0.11 kcal mol^{-1}), possibly due to its inclusion of single excitations which partly account for orbital relaxation.

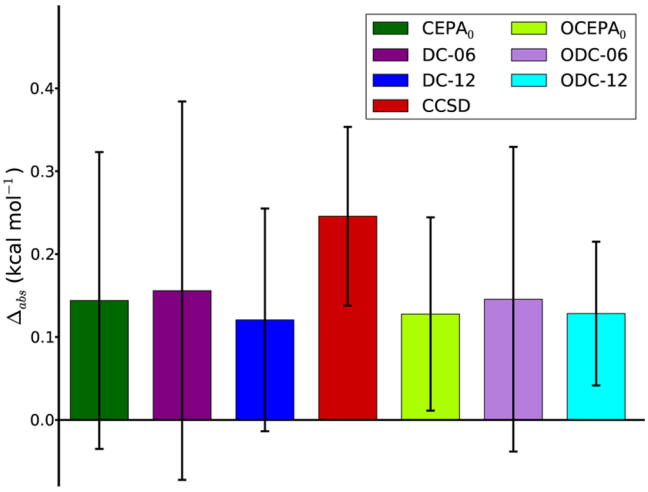

Figure 1. Mean absolute deviations (Δ_{abs}, kcal mol^{-1}) and the standard deviations from the mean signed error (Δ_{std}, kcal mol^{-1}) of the interaction energies for 24 noncovalently bound molecular dimers (A24 database) computed using seven methods with the aug-cc-pVTZ basis set. The errors are relative to CCSD(T)/aug-cc-pVTZ reference values. The Δ_{abs} value is represented as a height of each colored box, while the Δ_{std} value is depicted as a radius of the black vertical bar. See Table 1 for data on individual database members.

Errors in interaction energy and CCSD(T) reference values for each molecular complex are shown in Table 1. The largest deviations from CCSD(T) were obtained for the formaldehyde dimer ($CH_2O\cdots CH_2O$, complex 9 in Table 1), for which DC-06, $CEPA_0$, and $OCEPA_0$ yield errors of 0.99, 0.89, and 0.87 kcal mol^{-1}, respectively. For this system, the best performance is shown by CCSD and ODC-12, both of which give an error of 0.46 kcal mol^{-1}. For systems with π-stacking interactions (complexes 22−24 in Table 1), CCSD shows large errors (0.38, 0.43, 0.34) relative to the magnitude of the interaction energy (0.43, 0.41, 0.91 kcal mol^{-1}, respectively). Here $CEPA_0$, DC-12, and their orbital-optimized variants offer much better agreement with CCSD(T), with errors ranging from 0.01 to 0.15 kcal mol^{-1}.

Hydrogen-Transfer Reaction Barrier Heights. We continue by assessing the performance of DCFT methods in predicting barrier heights for 18 hydrogen-transfer reactions from the HTBH38 database:[61]

dx.doi.org/10.1021/ct5002895 | J. Chem. Theory Comput. XXXX, XXX, XXX−XXX

Table 2. Errors in Barrier Heights (kcal mol^{-1}) for 18 Hydrogen-Transfer Reactions ($R_1 + R_2H \rightarrow R_1H + R_2$) Comprising the HTBH38 Database[63] Computed Using Five Methods with the aug-cc-pVTZ Basis Set[a]

	reaction	ΔCEPA$_0$	ΔDC-12	ΔCCSD	ΔOCEPA$_0$	ΔODC-12	E_{ref} [CCSD(T)]
1	$H + HCl \rightarrow [HHCl]^* \rightarrow H_2 + Cl$	0.74	0.49	0.09	−0.41	−0.28	5.22
		1.44	1.31	1.61	0.53	0.77	7.39
2	$OH + H_2 \rightarrow [OHH_2]^* \rightarrow H + H_2O$	3.77	3.38	1.82	0.88	1.24	4.99
		2.09	1.66	0.09	−0.91	−0.58	21.07
3	$CH_3 + H_2 \rightarrow [CH_3H_2]^* \rightarrow H + CH_4$	1.60	1.46	1.37	0.46	0.70	11.29
		0.95	0.80	0.38	−0.38	−0.11	14.91
4	$OH + CH_4 \rightarrow [OHCH_4]^* \rightarrow CH_3 + H_2O$	4.26	3.85	2.61	1.22	1.65	5.64
		3.23	2.80	1.87	0.27	0.65	18.09
5	$H + H_2 \rightarrow [HH_2]^* \rightarrow H_2 + H$	0.80	0.69	0.30	−0.27	−0.05	9.77
6	$OH + NH_3 \rightarrow [OHNH_3]^* \rightarrow H_2O + NH_2$	6.02	5.25	3.54	1.18	1.82	3.17
		5.46	4.62	3.14	0.79	1.33	13.17
7	$HCl + CH_3 \rightarrow [HClCH_3]^* \rightarrow Cl + CH_4$	1.93	1.78	1.79	0.68	0.92	0.10
		1.97	1.94	2.31	0.78	1.16	5.89
8	$OH + C_2H_6 \rightarrow [OHC_2H_6]^* \rightarrow H_2O + C_2H_5$	4.66	4.21	2.69	1.28	1.72	2.69
		3.34	2.89	1.85	0.28	0.64	18.49
9	$F + H_2 \rightarrow [FH_2]^* \rightarrow HF + H$	3.40	3.14	1.20	0.52	0.78	1.13
		1.27	0.88	−0.78	−1.47	−1.33	32.95
10	$O + CH_4 \rightarrow [OHCH_3]^* \rightarrow OH + CH_3$	3.40	3.12	2.37	0.70	1.20	13.62
		2.62	2.29	1.82	0.32	0.68	7.43
11	$H + PH_3 \rightarrow [HPH_3]^* \rightarrow PH_2 + H_2$	0.93	0.86	0.59	−0.16	0.10	2.29
		1.14	1.11	1.37	0.39	0.63	23.21
12	$H + HO \rightarrow [OHH]^* \rightarrow H_2 + O$	2.03	1.59	0.44	−0.61	−0.26	10.25
		3.47	3.08	1.99	0.62	1.07	12.81
13	$H + H_2S \rightarrow [HH_2S]^* \rightarrow H_2 + HS$	1.01	0.92	0.65	−0.11	0.14	3.17
		1.51	1.51	1.88	0.65	0.97	16.41
14	$O + HCl \rightarrow [OHCl]^* \rightarrow OH + Cl$	6.33	6.01	3.58	0.79	1.51	9.74
		5.59	5.35	3.55	0.51	1.24	9.35
15	$NH_2 + CH_3 \rightarrow [CH_3NH_2]^* \rightarrow CH_4 + NH$	2.48	2.22	1.99	0.49	0.86	7.66
		2.77	2.49	2.26	0.73	1.12	21.32
16	$NH_2 + C_2H_5 \rightarrow [NH_2C_2H_5]^* \rightarrow C_2H_6 + NH$	2.48	2.22	2.09	0.55	0.92	8.21
		3.06	2.75	2.46	0.85	1.26	18.52
17	$C_2H_6 + NH_2 \rightarrow [C_2H_6NH_2]^* \rightarrow NH_3 + C_2H_5$	3.30	3.00	2.73	1.23	1.62	10.39
		2.54	2.30	2.30	0.63	1.02	16.20
18	$NH_2 + CH_4 \rightarrow [NH_2CH_4]^* \rightarrow CH_3 + NH_3$	2.98	2.72	2.55	1.11	1.48	13.23
		2.51	2.29	2.21	0.56	0.96	15.69
	Δ_{abs}	2.77	2.49	1.84	0.67	0.94	
	Δ_{std}	1.51	1.39	1.06	0.62	0.71	
	Δ_{rel}, %	99	90	77	29	40	

[a]The errors are relative to CCSD(T) reference values (E_{ref}, kcal mol^{-1}) shown in the rightmost column. For each reaction the first and the second lines present barrier heights in the forward ($R_1 + R_2H \rightarrow [R_1R_2H]^*$) and the backward ($[R_1R_2H]^* \rightarrow R_1H + R_2$) directions, respectively. The mean absolute (Δ_{abs}, kcal mol^{-1}) and the mean percent (Δ_{rel}, %) errors with respect to CCSD(T), as well as the standard deviations from the mean signed error (Δ_{std}, kcal mol^{-1}) are also shown.

$$R_1 + R_2H \rightarrow [R_1R_2H]^* \rightarrow R_1H + R_2 \quad (5)$$

These reactions [Reaction 19 in HTBH38, the cis−trans isomerization of piperylene, is omitted in the present study.] involve molecules (R_1 and R_2) and transition states ($[R_1R_2H]^*$) with open-shell character, making their properties more sensitive to electron correlation effects. We employ barrier heights computed at the CCSD(T)/aug-cc-pVTZ level of theory as our reference rather than the values provided by Lynch[63] in order to effectively exclude basis-set incompleteness effects. We also omit the DC-06 and ODC-06 methods, which encounter frequent convergence problems due to the poor description of *N*-representability (see the Supporting Information for incomplete DC-06 results).

Mean absolute deviations (Δ_{abs}) and standard deviations (Δ_{std}) for the hydrogen-transfer barrier heights are presented in Table 2 and plotted in Figure 2. The largest Δ_{abs} values come from CEPA$_0$ and DC-12 (2.77 and 2.49 kcal mol^{-1}, respectively). Orbital optimization greatly improves the accuracy of these methods, resulting in Δ_{abs} values of just 0.67 and 0.94 kcal mol^{-1} for OCEPA$_0$ and ODC-12, respectively. The CCSD method shows intermediate performance with Δ_{abs} = 1.84 kcal mol^{-1}. A similar trend is observed for the Δ_{std} values, with OCEPA$_0$ (0.62 kcal mol^{-1}) and ODC-12 (0.71 kcal mol^{-1}) significantly improving upon CEPA$_0$ (1.51 kcal mol^{-1}), DC-12 (1.39 kcal mol^{-1}), and CCSD (1.06 kcal mol^{-1}). In addition to Δ_{abs} and Δ_{std}, Table 2 includes mean percent error (Δ_{rel}) values, which are commonly used to benchmark performance for reaction kinetics. The smallest Δ_{rel}

dx.doi.org/10.1021/ct5002895 | J. Chem. Theory Comput. XXXX, XXX, XXX−XXX

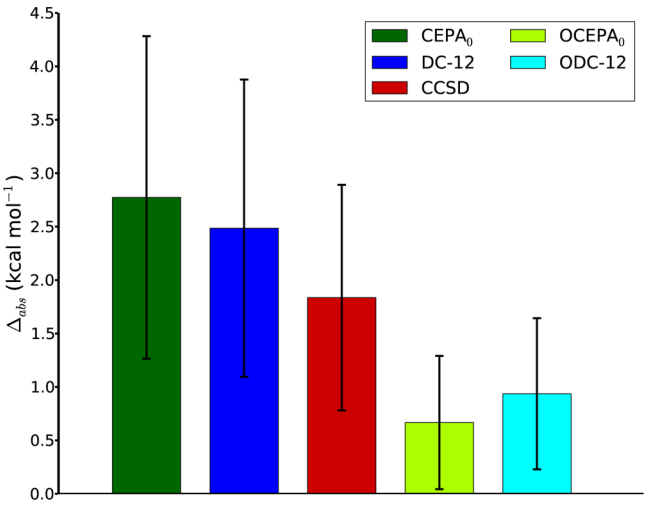

Figure 2. Mean absolute deviations (Δ_{abs}, kcal mol^{-1}) and the standard deviations from the mean signed error (Δ_{std}, kcal mol^{-1}) of barrier heights for 18 hydrogen-transfer reactions ($R_1 + R_2H \rightarrow R_1H + R_2$, HTBH38 database) computed using five methods with the aug-cc-pVTZ basis set. The errors are relative to CCSD(T)/aug-cc-pVTZ reference values. The Δ_{abs} value is represented as a height of each colored box, while the Δ_{std} value is depicted as a radius of the black vertical bar. See Table 2 for data on individual database members.

values are 29% and 40% for $OCEPA_0$ and ODC-12, respectively.

Turning to barrier heights for individual hydrogen-transfer reactions (Table 2), the largest errors are observed for reactions 6 and 14, both involving the OH radical, for which $CEPA_0$ and DC-12 give errors of ∼ 5−6 kcal mol^{-1}. The best results for these reactions are obtained from $OCEPA_0$, with errors ranging from 0.51 to 1.18 kcal mol^{-1}. The ODC-12 method tends to predict larger barrier heights than $OCEPA_0$, yielding smaller errors only when $OCEPA_0$ underestimates the barrier heights.

Radical Stabilization Energies. In this section we study the performance of DCFT methods for predicting radical stabilization energies (RSEs). An R-group's RSE is defined as the enthalpy of a homodesmotic reaction

$$RH + {}^{\bullet}CH_3 \rightarrow {}^{\bullet}R + CH_4 \qquad (6)$$

where exothermic (negative) values indicate that the radical $^{\bullet}R$ is more thermodynamically stable than $^{\bullet}CH_3$.[64] For our benchmark we use the RSE30 data set,[62] which provides a diverse variety of $^{\bullet}R$ species (listed in Table 3). Since the performance of CCSD(T) is known to deteriorate for strongly spin-contaminated UHF references,[65−69] we augment CCSD(T) energies with a quadruples correction ($\Delta Q = E_{CCSDT(Q)} - E_{CCSD(T)}$) and use these as our benchmark. CBS-extrapolated CCSD(T) reference values have been published for this data set,[30] but we use CCSD(T) values computed with the cc-pCVTZ basis set to avoid basis-set incompleteness effects. The ΔQ correction was evaluated using the cc-pCVDZ basis set. As in the previous section, DC-06 and ODC-06 computations cannot be converged for all database members and are omitted in the analysis below (see the Supporting Information for incomplete DC-06 and ODC-06 data).

The relative performance of the DCFT, CEPA, and CC methods for the RSE30 data set is shown in Figure 3. The effect of orbital-optimization on accuracy is now even more pronounced, reducing the large Δ_{abs} errors of $CEPA_0$ (2.97 kcal mol^{-1}) and DC-12 (2.01 kcal mol^{-1}) to 0.40 and 0.43 kcal mol^{-1} for $OCEPA_0$ and ODC-12, respectively. CCSD has a slightly larger value (0.62 kcal mol^{-1}), while CCSD(T) has the smallest overall Δ_{abs} (0.25 kcal mol^{-1}). Both $CEPA_0$ and DC-12 show large standard deviations again (3.97 and 2.27 kcal mol^{-1}, respectively). For $OCEPA_0$, the standard deviation (0.43 kcal mol^{-1}) is similar to that of CCSD (0.45 kcal mol^{-1}). ODC-12 and CCSD(T) exhibit the most consistent performance with the same Δ_{std} value of 0.35 kcal mol^{-1}.

Deviations from CCSD(T)+ΔQ for individual RSEs predicted by each method are tabulated in Table 3. In addition, Table 3 includes expectation values of the square-norm spin operator computed for the UHF wave function of $^{\bullet}R$ ($\langle \hat{S}^2 \rangle_{SCF}$). The largest errors in computed RSEs were obtained for $^{\bullet}R$ species with $\langle \hat{S}^2 \rangle_{SCF} > 0.9\ \hbar^2$ (radicals 4, 6, 7, 16, and 27−30 in Table 3). For these systems, the average $CEPA_0$ and DC-12 errors are 8.05 and 4.72 kcal mol^{-1} and the average CCSD(T) error is 0.68 kcal mol^{-1}. $OCEPA_0$ and ODC-12 offer remarkably better performance for this subset, with average errors of 0.24 kcal mol^{-1} and 0.26 kcal mol^{-1}

Adiabatic Ionization Energies in Electron-Dense Molecules. We conclude the assessment of DCFT methods for the description of thermodynamic properties by computing adiabatic ionization energies (AIEs) for a set of 10 di- and triatomic electron-dense molecules (Table 4), i.e. those that are composed of elements with small atomic radius, high electron affinity, and high electronegativity (N, O, F), in order to increase the magnitude of electron correlation effects. We use experimentally measured ionization energies reported to high precision (∼0.01 eV)[70−73] as reference values for our benchmark (IE_{ref}, Table 4). The AIEs were computed using the cc-pCVQZ basis set, with harmonic ZPVE corrections applied to each neutral and cationic system.

The Δ_{abs} and Δ_{std} values for our computed AIEs relative to experiment are plotted in Figure 4. Of the six methods, $CEPA_0$ and DC-12 exhibit the largest Δ_{abs} values (0.21 and 0.13 eV, respectively). The closest agreement with experiment is given by ODC-12, with Δ_{abs} = 0.03 eV. $OCEPA_0$, CCSD, and CCSD(T) show somewhat poorer performance (Δ_{abs} = 0.05, 0.06, and 0.06 eV, respectively). The Δ_{std} for ODC-12 matches that of CCSD(T) (0.04 eV). For the other methods, the Δ_{std} values decrease in the order $CEPA_0$ (0.22 eV) > DC-12 (0.12) > CCSD (0.08) > $OCEPA_0$ (0.06).

Individual errors for each system are shown in Table 4. Both DC-12 and $CEPA_0$ exhibit large deviations for F_2O (0.49 and 0.37 eV), and $CEPA_0$ also gives a large error for FNO (0.51 eV) which is the maximum error for this data set. Both DC-12 and $CEPA_0$ give errors exceeding 0.1 eV for seven of the ten systems, whereas CCSD exhibits errors in excess of 0.1 eV for only three systems (OF, HNC, and HOF). CCSD(T) has only one such error (0.11 eV for OF), as does $OCEPA_0$ (0.14 eV for HNC). ODC-12 does the best of the methods considered, with a maximum error of 0.08 eV, found for the AIE of HNC.

Covalent Bond Stretching in Diatomic Molecules. Finally, we benchmark DCFT methods for covalent bond stretching. Although accurate description of bond stretching demands the use of multireference methods, our aim here is to explore the limits of DCFT away from equilibrium. For this purpose, we compute the energy as a function of bond distance for diatomic molecules with single (HF and BH), double (BeO), and triple (N_2) bonds using the $CEPA_0$, $OCEPA_0$, DC-12, ODC-12, CCSD, and CCSD(T) methods. We restrict ourselves to modest basis sets in order to use full CI (FCI) as a reference, and plot the errors with respect to FCI (ΔE) as a

dx.doi.org/10.1021/ct5002895 | J. Chem. Theory Comput. XXXX, XXX, XXX−XXX

Table 3. Errors in Radical Stabilization Energies (RSEs, kcal mol^{-1}) for 30 Open-Shell Doublet Species ($^{\bullet}$R) Comprising the RSE30 Database[62] Computed Using Six Methods with the cc-pCVTZ Basis Set[a]

	$^{\bullet}$R	$\langle\hat{S}^2\rangle^{SCF}$	ΔCEPA$_0$	ΔDC-12	ΔCCSD	ΔOCEPA$_0$	ΔODC-12	ΔCCSD(T)	E_{ref} [CCSD(T)+ΔQ]
1	$^{\bullet}CH_2NO_2$	0.78	1.24	0.95	0.66	0.16	0.27	0.32	−3.50
2	$^{\bullet}CH_2OCHO$	0.76	1.16	1.12	0.63	0.40	0.48	0.10	−4.84
3	$^{\bullet}CH_2SCH_3$	0.76	1.89	1.70	0.81	0.63	0.72	0.15	−11.01
4	$^{\bullet}CF{=}CH_2$	0.94	6.12	3.71	0.96	0.42	0.64	0.46	6.26
5	$^{\bullet}CH_2CH_2F$	0.76	0.30	0.27	0.13	0.08	0.10	0.04	−1.53
6	$^{\bullet}CH_2CHO$	0.93	5.01	2.86	0.32	−0.16	0.02	0.46	−10.11
7	$^{\bullet}CH_2CN$	0.94	6.36	3.52	0.65	−0.02	0.21	0.46	−8.66
8	$^{\bullet}CH_2F$	0.76	1.03	1.00	0.52	0.55	0.57	0.06	−4.22
9	$^{\bullet}CH_2NH_2$	0.76	1.28	1.18	0.59	0.50	0.52	0.06	−12.06
10	$^{\bullet}CH_2NH_3^+$	0.76	0.16	0.10	0.08	0.06	0.03	0.02	4.58
11	$^{\bullet}CH_2NHOH$	0.77	1.76	1.57	0.78	0.58	0.64	0.15	−8.81
12	$^{\bullet}CH_2OH$	0.76	1.29	1.23	0.62	0.57	0.60	0.07	−9.27
13	$^{\bullet}CH_2PH_3^+$	0.76	0.21	0.14	0.01	0.01	−0.02	0.05	0.49
14	$^{\bullet}CH_2SH_2^+$	0.77	0.41	0.30	0.12	0.11	0.08	0.06	2.29
15	$^{\bullet}CH_2SH$	0.76	1.60	1.43	0.68	0.57	0.63	0.12	−9.68
16	$^{\bullet}CH_2C{\equiv}CH$	1.00	6.23	3.47	0.82	−0.03	0.23	0.52	−13.17
17	$^{\bullet}CH_2CH_3$	0.76	0.30	0.26	0.11	0.08	0.10	0.03	−3.36
18	$^{\bullet}CH_2Cl$	0.77	1.13	1.02	0.50	0.48	0.51	0.09	−5.67
19	$^{\bullet}CH_2BH_2$	0.76	0.17	0.17	0.05	0.03	0.04	0.05	−11.66
20	$^{\bullet}CHO$	0.77	2.26	2.24	1.48	1.55	1.56	0.20	−17.61
21	$^{\bullet}CH_2PH_2$	0.76	1.17	1.02	0.39	0.36	0.39	0.12	−6.50
22	$^{\bullet}CHClF$	0.76	1.61	1.52	0.76	0.78	0.81	0.13	−6.61
23	$^{\bullet}CHFCH_3$	0.76	1.07	1.01	0.50	0.51	0.53	0.08	−5.87
24	$^{\bullet}CH(OH)_2$	0.76	1.30	1.22	0.60	0.60	0.61	0.08	−6.67
25	$^{\bullet}CHCl_2$	0.77	1.78	1.57	0.72	0.72	0.75	0.15	−9.56
26	$^{\bullet}CHF_2$	0.76	1.50	1.48	0.78	0.83	0.85	0.10	−4.07
27	$CH_2{=}C^{\bullet}{-}CN$	1.39	19.10	11.50	2.36	−0.31	0.29	1.80	1.98
28	$^{\bullet}C{\equiv}CH$	1.15	11.20	6.51	0.77	−0.78	−0.07	0.82	26.25
29	$^{\bullet}CH{=}CH_2$	0.94	5.42	3.01	0.58	0.11	0.31	0.40	5.49
30	$^{\bullet}CH_2{-}CH{=}CH_2$	0.97	4.98	3.17	0.51	0.11	0.31	0.48	−17.53
		Δ_{abs}	2.97	2.01	0.62	0.40	0.43	0.25	
		Δ_{std}	3.97	2.27	0.45	0.43	0.35	0.35	

[a]The errors are relative to CCSD(T) with an added quadruples correction ($\Delta Q = E_{CCSDT(Q)} - E_{CCSD(T)}$) shown in the rightmost column (E_{ref}, kcal mol^{-1}). The ΔQ correction was computed using the cc-pCVDZ basis set. RSE is defined as the reaction enthalpy for the homodesmotic reaction $^{\bullet}CH_3 + RH \rightarrow CH_4 + {}^{\bullet}R$. To indicate the degree of spin-contamination in the UHF reference, the $\hat{S}^2$ expectation values ($\langle\hat{S}^2\rangle_{SCF}$) are also shown in units of $\hbar^2$. For each method the mean absolute deviations from CCSD(T)+ΔQ (Δ_{abs}, kcal mol^{-1}) and the standard deviations from the mean signed error (Δ_{std}, kcal mol^{-1}) are also presented.

function of internuclear distance for each molecule. The relative performance of the methods is described below using non-parallelity errors (NPE = $\Delta E_{max} - \Delta E_{min}$, m$E_h$) computed for specific bond distance ranges.

BH. Figure 5 shows errors relative to FCI for the BH molecule. DC-12 and CCSD increasingly overestimate the energy at larger internuclear distances, whereas the CEPA$_0$ error curve is concave down. Orbital optimization lowers the binding energy for OCEPA$_0$ even further compared to CEPA$_0$, leading to large errors with respect to FCI for r(B−H) > 1.5 r_e, where r_e is the FCI equilibrium bond distance (r_e = 1.244 Å). At 1.87 r_e, OCEPA$_0$ encounters convergence problems, which originate from numerical instabilities due to the method's deficiencies in the description of *N*-representability. The ODC-12 method exhibits much more stable behavior with respect to bond stretching in this case, fortuitously showing smaller errors and better parallelity than CCSD(T). For the range [0.72 r_e, 2.47 r_e], the NPEs decrease in the order DC-12 (24 mE_h) > CEPA$_0$ (15) > CCSD (5) > CCSD(T) (3) > ODC-12 (1).

HF. Errors for HF bond stretching are plotted in Figure 6. The Δ*E* values of CCSD and DC-12 increase as a function of r(H−F), while CEPA$_0$ fortuitously maintains parallelity similar to CCSD(T) over the range [0.74 r_e, 1.94 r_e] (r_e = 0.929 Å). OCEPA$_0$ increasingly overestimates the HF binding energy away from equilibrium, failing to converge past 1.82 r_e. The ODC-12 method exhibits larger NPE than was observed for BH, and encounters convergence problems past 1.94 r_e. CCSD(T) shows the best overall performance, with errors between 0 and 1 mE_h. In the range [0.74 r_e, 1.94 r_e] the computed NPE values are DC-12 (15 mE_h) > CCSD (7) > ODC-12 (3) > CEPA$_0$ (1) ≈ CCSD(T) (1). Recently, the orbital-optimized variants of CCSD(T) have been shown to yield good performance for HF bond stretching.[74]

BeO. The double bond of BeO presents a more challenging test for the single-reference methods under consideration (Figure 7). All methods but CCSD(T) show qualitatively similar error curves, with inflection points near the FCI equilibrium (r_e = 1.394 Å) and valleys/peaks around 0.6 r_e/1.2

dx.doi.org/10.1021/ct5002895 | J. Chem. Theory Comput. XXXX, XXX, XXX−XXX

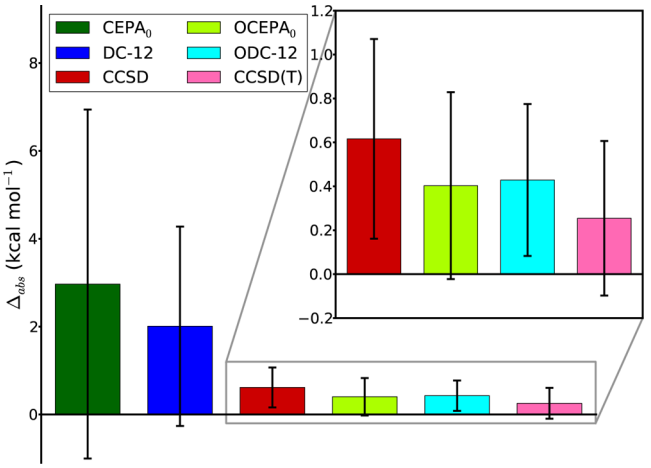

Figure 3. Mean absolute deviations (Δ_{abs}, kcal mol^{-1}) and the standard deviations from the mean signed error (Δ_{std}, kcal mol^{-1}) of the radical stabilization energies (RSEs) for 30 open-shell doublet species (RSE30 database) computed using six methods with the cc-pCVTZ basis set. The errors are relative to CCSD(T) with an added quadruples correction ($\Delta Q = E_{CCSDT(Q)} - E_{CCSD(T)}$). The ΔQ correction was computed using the cc-pCVDZ basis set. RSE is defined as the reaction enthalpy for the homodesmotic reaction $^{\bullet}CH_3 + RH \rightarrow CH_4 + {}^{\bullet}R$. The Δ_{abs} value is represented as a height of each colored box, while the Δ_{abs} value is depicted as a radius of the black vertical bar. See Table 3 for data on individual database members.

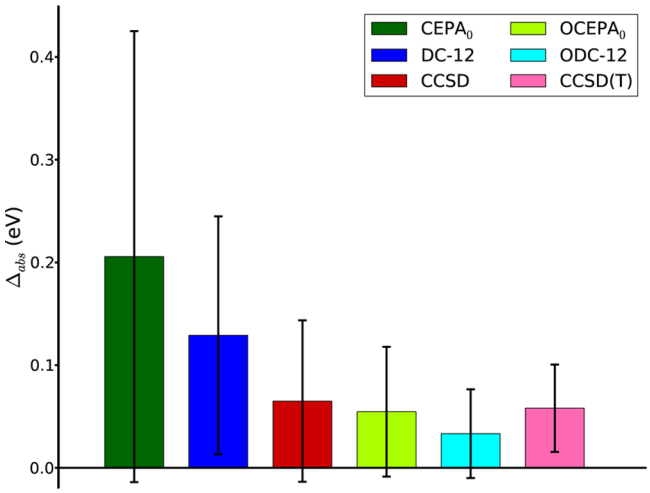

Figure 4. Mean absolute deviations (Δ_{abs}, eV) and the standard deviations from the mean signed error (Δ_{std}, eV) of adiabatic ionization energies for 10 di- and triatomic molecules computed using six methods with the cc-pCVQZ basis set. The errors are relative to experimental values.[70−73] The Δ_{abs} value is represented as a height of each colored box, while the Δ_{std} value is depicted as a radius of the black vertical bar. See Table 4 for data on individual molecules.

r_e. OCEPA$_0$ encounters convergence problems past 1.10r_e. The ODC-12 method performs similarly to CCSD. Overall, the NPEs for the range [0.65 r_e, 1.10 r_e] decrease in the following order: DC-12 (29 mE_h) > CEPA$_0$ (24) > ODC-12 (19) > CCSD (17) > CCSD(T) (3).

N_2. Figure 8 depicts the errors relative to FCI for triple bond stretching in N_2. Here, OCEPA$_0$ fails to converge past 1.24 r_e (r_e = 1.135 Å). The ODC-12 method significantly overestimates the binding energy, possibly due to the lack of three-body correlation effects but shows much more stable performance compared to methods other than CCSD(T). NPEs in the range [0.79 r_e, 1.39 r_e] decrease in the order: CEPA$_0$ (802 mE_h) [CEPA$_0$ exhibits a vertical asymptote at 1.36 r_e for N_2 stretching.] > CCSD (27) > DC-12 (21) > ODC-12 (14) > CCSD(T) (4).

CONCLUSIONS

We have presented the benchmark study of four density cumulant functional theory (DCFT) methods (DC-06, DC-12, ODC-06, and ODC-12) developed recently in our group.[48,49,51,52] Specifically we have compared the performance of DCFT to that of coupled electron pair methods (CEPA$_0$ and OCEPA$_0$), as well as coupled-cluster theory [CCSD and CCSD(T)] for predicting a variety of chemical properties relevant to thermochemistry and kinetics, with a particular focus on open-shell, electron-dense, and nonequilibrium systems.

Our results indicate that among the four DCFT methods, the best agreement with available reference data is obtained for the

Table 4. Errors in Adiabatic Ionization Energies (AIEs, eV) for 10 Di- and Triatomic Molecules Computed Using Six Methods with the cc-pCVQZ Basis Set[a]

molecule	electronic transition	ΔCEPA$_0$	ΔDC-12	ΔCCSD	ΔOCEPA$_0$	ΔODC-12	ΔCCSD(T)	IE$_{ref}$
N_2	$^1\Sigma_g^+ \rightarrow {}^2\Sigma_g^+$	0.08	0.17	0.12	−0.05	0.07	−0.03	15.581 ± 0.008[b]
O_2	$3\Sigma_g^- \rightarrow {}^2\Pi_g$	−0.11	−0.03	0.04	−0.09	−0.02	−0.04	12.0697 ± 0.0002
F_2	$^1\Sigma_g^+ \rightarrow {}^2\Pi_g$	0.06	0.06	0.04	0.08	0.01	−0.03	15.697 ± 0.003
NO	$^2\Pi \rightarrow {}^1\Sigma^+$	−0.15	−0.05	−0.05	−0.05	−0.02	−0.09	9.26438 ± 0.00005
OF	$^2\Pi \rightarrow {}^3\Sigma^-$	0.11	0.12	−0.10	−0.03	−0.02	−0.11	12.77 ± 0.01[c]
HNC	$^1\Sigma^+ \rightarrow {}^2\Sigma^+$	0.27	0.14	−0.12	−0.14	−0.08	−0.04	12.04 ± 0.01[d]
HOF	$^1A' \rightarrow {}^2A''$	0.20	0.17	−0.10	−0.03	−0.04	−0.07	12.71 ± 0.01
FNO	$^1A' \rightarrow {}^2A''$	0.51	0.10	−0.02	−0.02	−0.00	0.04	12.63 ± 0.03
F_2N	$^2B_1 \rightarrow {}^1A_1$	0.07	0.10	0.07	0.01	0.03	−0.08	11.63 ± 0.01
F_2O	$^1A_1 \rightarrow {}^2B_1$	0.49	0.37	−0.01	0.05	0.04	−0.04	13.11 ± 0.01
	Δ_{abs}	0.21	0.13	0.06	0.05	0.03	0.06	
	Δ_{std}	0.22	0.12	0.08	0.06	0.04	0.04	

[a]The errors are relative to experimental values (IE$_{ref}$, eV) from ref 70, unless noted otherwise. For all AIEs, the harmonic zero-point vibrational energy corrections were included. For each method the mean absolute deviations from IE$_{ref}$ (Δ_{abs}, eV) and the standard deviations from the mean signed error (Δ_{std}, eV) are also shown. [b]Reference 71. [c]Reference 72. [d]Reference 73.

dx.doi.org/10.1021/ct5002895 | J. Chem. Theory Comput. XXXX, XXX, XXX−XXX

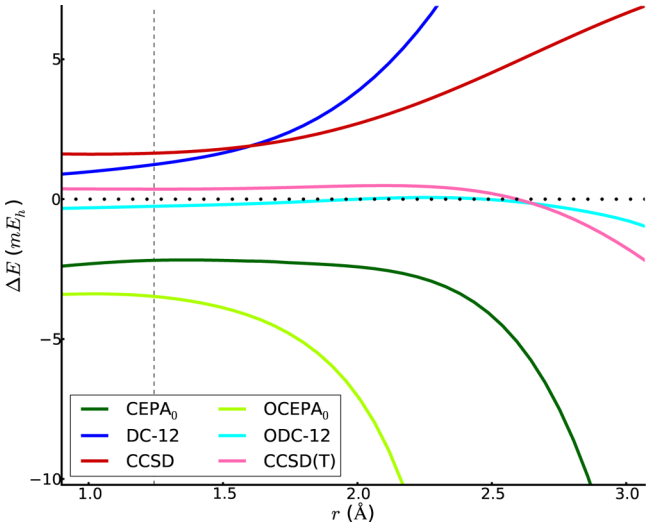

Figure 5. Error in the total energy (mE_h), relative to full CI, as a function of B−H internuclear separation (Å) computed using six methods with the DZP basis set. The full CI reference is depicted with a horizontal dotted line. The dashed vertical line indicates the full CI equilibrium bond distance.

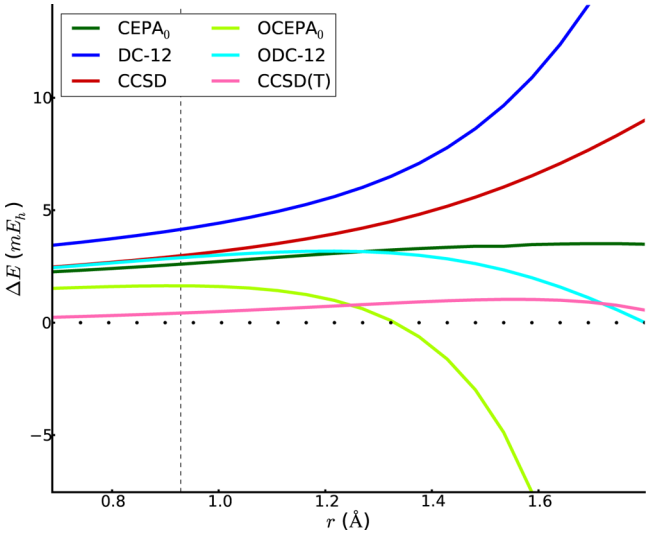

Figure 6. Error in the total energy (mE_h), relative to full CI, as a function of H−F internuclear separation (Å) computed using six methods with the DZP basis set. The full CI reference is depicted with a horizontal dotted line. The dashed vertical line indicates the full CI equilibrium bond distance.

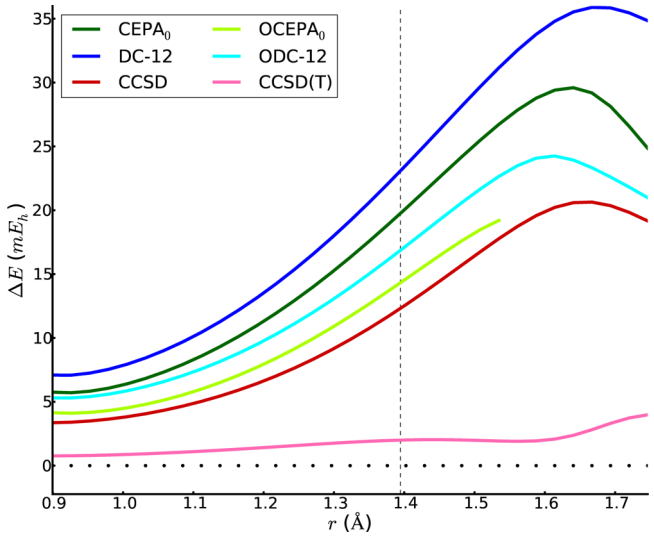

Figure 7. Error in the total energy (mE_h), relative to full CI, as a function of Be−O internuclear separation (Å) computed using six methods with the 6-31G basis set. The full CI reference is depicted with a horizontal dotted line. The dashed vertical line indicates the full CI equilibrium bond distance.

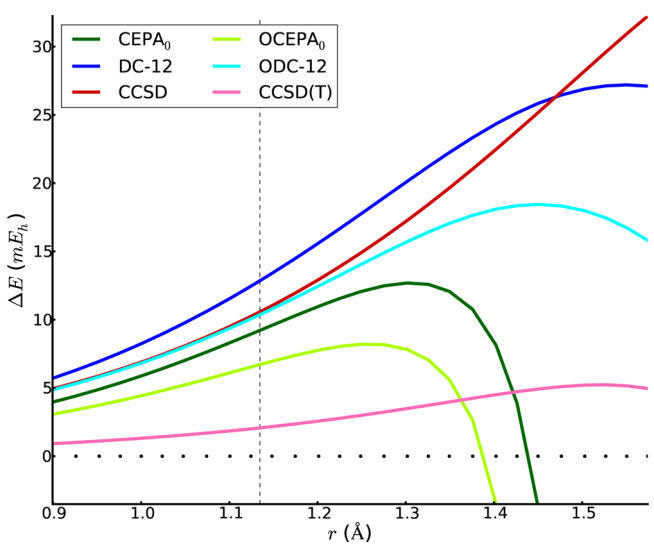

Figure 8. Error in the total energy (mE_h), relative to full CI, as a function of N−N internuclear separation (Å) computed using six methods with the 6-31G basis set. The full CI reference is depicted with a horizontal dotted line. The dashed vertical line indicates the full CI equilibrium bond distance.

ODC-12 method. While all four DCFT formulations yield similar results for the description of noncovalent interactions, DC-06, DC-12, and ODC-06 exhibit worse performance than ODC-12 for thermodynamic and kinetic properties of reactions involving open-shell molecules. In particular, DC-06 and ODC-06 frequently encounter convergence problems that originate from poor description of N-representability. In comparing ODC-12 to other methods, several trends can be observed:

(i) For all benchmark data sets, ODC-12 outperforms CCSD with errors smaller by almost a factor of 2, on average. ODC-12 is also superior to CCSD for the description of single bond stretching in BH and HF, although it does not converge for all bond distances.

(ii) The performance of ODC-12 and OCEPA$_0$ is comparable. In particular, for hydrogen-transfer reaction barrier heights, the OCEPA$_0$ method yields smaller percent errors than ODC-12, whereas, for the radical stabilization energies (RSE) and adiabatic ionization energies (AIE) in electron-dense molecules, the ODC-12 method shows smaller standard deviations than OCEPA$_0$. For AIEs, ODC-12 gives smaller mean absolute deviations by almost a factor of 2. ODC-12 also shows significantly smaller nonparallelity errors than OCEPA$_0$ for covalent bond stretching, and can be converged for a larger range of distances for all diatomic molecules studied.

dx.doi.org/10.1021/ct5002895 | J. Chem. Theory Comput. XXXX, XXX, XXX−XXX

(iii) For the two most challenging data sets, RSE and AIE, the standard deviation of ODC-12 and CCSD(T) are similar. While CCSD(T) yields smaller mean absolute errors for the RSE database, the ODC-12 method significantly outperforms CCSD(T) for the AIE test case. However, for bond stretching ODC-12 is competitive with CCSD(T) only for the BH dissociation and shows worse results for other molecules.

Overall, the data presented herein indicates that the ODC-12 method can be used as an efficient $O(n^6)$ alternative to CCSD, capable of predicting thermodynamic and kinetic quantities that are competitive in accuracy with the "gold-standard" $O(n^7)$ CCSD(T). Although our current implementation of ODC-12 is far from optimal, the ODC-12 equations have reduced nonlinearities compared to CCSD, which makes them more amenable to parallel implementation. The efficiency of ODC-12 can also greatly benefit from spin-adaptation,[41,75,76] local approximations,[33,77−79] and density fitting.[77,80−82] Another important advantage of ODC-12 over CCSD is its stationarity, which makes the computation of first-order properties and analytic gradients more efficient and easily accessible. In particular, ODC-12 has potential to be used for computing accurate response properties which do not suffer from a lack of gauge-invariance.[83,84]

■ ASSOCIATED CONTENT

Supporting Information

Tables presenting incomplete results for the HTBH38 and RSE30 databases computed using the DC-06 and ODC-06 methods. This material is available free of charge via the Internet at http://pubs.acs.org/.

■ AUTHOR INFORMATION

Corresponding Author

*E-mail: avcopan@uga.edu.

Notes

The authors declare no competing financial interest.

■ ACKNOWLEDGMENTS

This research was supported by the U.S. National Science Foundation (Grants No. CHE-1054286 and CHE-1361178). We acknowledge computing resources of Extreme Science and Engineering Discovery Environment (XSEDE, Grant No. TG-CHE130079). The authors thank Dr. Jay Agarwal for helpful discussions.

■ REFERENCES

(1) Nooijen, M.; Shamasundar, K. R.; Mukherjee, D. *Mol. Phys.* **2005**, *103*, 2277−2298.
(2) Pople, J. A.; Binkley, J. S.; Seeger, R. *Int. J. Quantum Chem.* **1976**, *10*, 1−19.
(3) Bartlett, R. J. *Annu. Rev. Phys. Chem.* **1981**, *32*, 359−401.
(4) Szalay, P. G.; Nooijen, M.; Bartlett, R. J. *J. Chem. Phys.* **1995**, *103*, 281−298.
(5) Kelly, H. P.; Sessler, A. M. *Phys. Rev.* **1963**, *132*, 2091−2095.
(6) Kelly, H. P. *Phys. Rev. A* **1964**, *134*, 1450−1453.
(7) Meyer, W. *J. Chem. Phys.* **1973**, *58*, 1017−1035.
(8) Ahlrichs, R. *Comput. Phys. Commun.* **1979**, *17*, 31−45.
(9) Koch, S.; Kutzelnigg, W. *Theor. Chim. Acta* **1981**, *59*, 387−411.
(10) Gelus, M.; Ahlrichs, R.; Staemmler, V.; Kutzelnigg, W. *Chem. Phys. Lett.* **1970**, *7*, 503−505.
(11) Staemmler, V.; Jungen, M. *Chem. Phys. Lett.* **1972**, *16*, 187−191.
(12) Ahlrichs, R.; Driessler, F.; Lischka, H.; Staemmler, V.; Kutzelnigg, W. *J. Chem. Phys.* **1975**, *62*, 1235−1247.
(13) Kollmar, H.; Staemmler, V. *J. Am. Chem. Soc.* **1977**, *99*, 3583−3587.
(14) Wasilewski, J.; Staemmler, V.; Koch, S. *Phys. Rev. A* **1988**, *38*, 1289−1299.
(15) Taube, A. G.; Bartlett, R. J. *J. Chem. Phys.* **2009**, *130*, 144112.
(16) Coester, F. *Nucl. Phys.* **1958**, *7*, 421−424.
(17) Coester, F.; Kümmel, H. *Nucl. Phys.* **1960**, *17*, 477−485.
(18) Čížek, J. *J. Chem. Phys.* **1966**, *45*, 4256−4266.
(19) Bartlett, R. J.; Purvis, G. D. *Int. J. Quantum Chem.* **1978**, *14*, 561−581.
(20) Crawford, T. D.; Schaefer, H. F. *Rev. Comp. Chem.* **2000**, *14*, 33−136.
(21) Bartlett, R. J.; Musiał, M. *Rev. Mod. Phys.* **2007**, *79*, 291−352.
(22) Shavitt, I.; Bartlett, R. J. *Many-Body Methods in Chemistry and Physics*; Cambridge University Press: Cambridge, UK, 2009.
(23) Kollmar, C.; Neese, F. *Mol. Phys.* **2010**, *108*, 2449−2458.
(24) Daudey, J. P.; Heully, J. L.; Malrieu, J. P. *J. Chem. Phys.* **1993**, *99*, 1240−1254.
(25) Malrieu, J. P.; Zhang, H.; Ma, J. *Chem. Phys. Lett.* **2010**, *493*, 179−184.
(26) Nooijen, M.; Le Roy, R. J. *J. Mol. Struct.* **2006**, *768*, 25−43.
(27) Kollmar, C.; Neese, F. *J. Chem. Phys.* **2011**, *135*, 84102.
(28) Kollmar, C.; Heßelmann, A. *Theor. Chem. Acc.* **2010**, *127*, 311−325.
(29) Bozkaya, U.; Sherrill, C. D. *J. Chem. Phys.* **2013**, *139*, 054104.
(30) Soydaş, E.; Bozkaya, U. *J. Comput. Chem.* **2014**, *35*, 1073−1081.
(31) Bozkaya, U. *J. Chem. Phys.* **2013**, *139*, 154105.
(32) Wennmohs, F.; Neese, F. *Chem. Phys.* **2008**, *343*, 217−230.
(33) Neese, F.; Wennmohs, F.; Hansen, A. *J. Chem. Phys.* **2009**, *130*, 114108.
(34) Kutzelnigg, W. *J. Chem. Phys.* **2006**, *125*, 171101.
(35) Mazziotti, D. A. *Phys. Rev. Lett.* **2008**, *101*, 253002.
(36) Mazziotti, D. A. *Phys. Rev. A* **2010**, *81*, 62515.
(37) DePrince, A. E.; Mazziotti, D. A. *Mol. Phys.* **2012**, *110*, 1917−1925.
(38) Kutzelnigg, W.; Mukherjee, D. *J. Chem. Phys.* **1997**, *107*, 432−449.
(39) Mazziotti, D. A. *Chem. Phys. Lett.* **1998**, *289*, 419−427.
(40) Mazziotti, D. A. *Phys. Rev. A* **1998**, *57*, 4219−4234.
(41) Kutzelnigg, W.; Mukherjee, D. *J. Chem. Phys.* **1999**, *110*, 2800−2809.
(42) Kong, L. *Int. J. Quantum Chem.* **2011**, *111*, 3541−3547.
(43) Hanauer, M.; Köhn, A. *Chem. Phys.* **2012**, *401*, 50−61.
(44) Nakata, M.; Yasuda, K. *Phys. Rev. A* **2009**, *80*, 42109.
(45) van Aggelen, H.; Verstichel, B.; Bultinck, P.; Van Neck, D.; Ayers, P. W.; Cooper, D. L. *J. Chem. Phys.* **2010**, *132*, 114112.
(46) Verstichel, B.; van Aggelen, H.; Van Neck, D.; Ayers, P. W.; Bultinck, P. *J. Chem. Phys.* **2010**, *132*, 114113.
(47) Herbert, J. M.; Harriman, J. E. *Adv. Chem. Phys.* **2007**, *134*, 261−292.
(48) Simmonett, A. C.; Wilke, J. J.; Schaefer, H. F.; Kutzelnigg, W. *J. Chem. Phys.* **2010**, *133*, 174122.
(49) Sokolov, A. Y.; Wilke, J. J.; Simmonett, A. C.; Schaefer, H. F. *J. Chem. Phys.* **2012**, *137*, 054105.
(50) Kutzelnigg, W.; Mukherjee, D. *J. Chem. Phys.* **2004**, *120*, 7350−7368.
(51) Sokolov, A. Y.; Simmonett, A. C.; Schaefer, H. F. *J. Chem. Phys.* **2013**, *138*, 024107.
(52) Sokolov, A. Y.; Schaefer, H. F. *J. Chem. Phys.* **2013**, *139*, 204110.
(53) Mazziotti, D. A., Ed. *Reduced-Density-Matrix Mechanics: With Application to Many-Electron Atoms and Molecules*; Advances in Chemical Physics; John Wiley & Sons, Inc.: Hoboken, NJ, 2007; Vol. *134*.
(54) Turney, J. M.; et al. *WIREs Comput. Mol. Sci.* **2012**, *2*, 556−565.
(55) Raghavachari, K.; Trucks, G. W.; Pople, J. A.; Head-Gordon, M. *Chem. Phys. Lett.* **1989**, *157*, 479−483.
(56) Stanton, J. F. *Chem. Phys. Lett.* **1997**, *281*, 130−134.

(57) Dunning, T. H. *J. Chem. Phys.* **1989**, *90*, 1007−1023.
(58) Woon, D. E.; Dunning, T. H. *J. Chem. Phys.* **1995**, *103*, 4572−4585.
(59) Kendall, R. A.; Dunning, T. H.; Harrison, R. J. *J. Chem. Phys.* **1992**, *96*, 6796−6806.
(60) Řezáč, J.; Hobza, P. *J. Chem. Theory Comput.* **2013**, *9*, 2151−2155.
(61) Zhao, Y.; Lynch, B. J.; Truhlar, D. G. *Phys. Chem. Chem. Phys.* **2005**, *7*, 43−52.
(62) Soydas, E.; Bozkaya, U. *J. Chem. Theory Comput.* **2013**, *9*, 1452−1460.
(63) Lynch, B. J.; Zhao, Y.; Truhlar, D. G. The Minnesota Databases for Chemistry and Solid-State Physics. http://comp.chem.umn.edu/db/; accessed May 20, 2014.
(64) Zipse, H. *Top. Curr. Chem.* **2006**, *263*, 163−189.
(65) Byrd, E. F. C.; Sherrill, C. D.; Head-Gordon, M. *J. Phys. Chem. A* **2001**, *105*, 9736−9747.
(66) Beran, G. J. O.; Gwaltney, S. R.; Head-Gordon, M. *Phys. Chem. Chem. Phys.* **2003**, *5*, 2488.
(67) Lochan, R. C.; Head-Gordon, M. *J. Chem. Phys.* **2007**, *126*, 164101−164111.
(68) Kurlancheek, W.; Head-Gordon, M. *Mol. Phys.* **2009**, *107*, 1223−1232.
(69) Bozkaya, U. *J. Chem. Phys.* **2011**, *135*, 224103.
(70) Lias, S. G.; Bartmess, J. E.; Liebman, J. F.; Holmes, J. L.; Levin, R. D.; Mallard, W. G. *J. Phys. Chem. Ref. Data* **1988**, *17*, 1−861.
(71) Trickl, T.; Cromwell, E. F.; Lee, Y. T.; Kung, A. H. *J. Chem. Phys.* **1989**, *91*, 6006−6012.
(72) Zhang, Z.; Kuo, S. C.; Klemm, R. B.; Monks, P. S.; Stief, L. J. *Chem. Phys. Lett.* **1994**, *229*, 377−382.
(73) Hansel, A.; Scheiring, C.; Glantschnig, M.; Lindinger, W.; Ferguson, E. E. *J. Chem. Phys.* **1998**, *109*, 1748−1750.
(74) Bozkaya, U.; Schaefer, H. F. *J. Chem. Phys.* **2012**, *136*, 204114.
(75) Kutzelnigg, W.; Mukherjee, D. *J. Chem. Phys.* **2002**, *116*, 4787−4801.
(76) Kutzelnigg, W.; Shamasundar, K. R.; Mukherjee, D. *Mol. Phys.* **2010**, *108*, 433−451.
(77) Werner, H.-J.; Manby, F. R.; Knowles, P. J. *J. Chem. Phys.* **2003**, *118*, 8149−8160.
(78) Taube, A. G.; Bartlett, R. J. *Collect. Czech. Chem. Commun.* **2005**, *70*, 837−850.
(79) Neese, F.; Hansen, A.; Liakos, D. G. *J. Chem. Phys.* **2009**, *131*, 064103.
(80) Vahtras, O.; Almlöf, J.; Feyereisen, M. W. *Chem. Phys. Lett.* **1993**, *213*, 514−518.
(81) Hetzer, G.; Schütz, M.; Stoll, H.; Werner, H.-J. *J. Chem. Phys.* **2000**, *113*, 9443−9455.
(82) Schütz, M.; Werner, H.-J. *J. Chem. Phys.* **2001**, *114*, 661−681.
(83) Pedersen, T. B.; Koch, H.; Hättig, C. *J. Chem. Phys.* **1999**, *110*, 8318−8327.
(84) Pedersen, T. B.; Fernández, B.; Koch, H. *J. Chem. Phys.* **2001**, *114*, 6983−6993.